

# Influence of the metal complex-to-peptide linker on the synthesis and properties of bioactive CpMn(CO)<sub>3</sub> peptide conjugates†

Katrin Splith,<sup>a</sup> Ines Neundorff,<sup>\*a</sup> Wanning Hu,<sup>b</sup> Harmel W. Peindy N'Dongo,<sup>b</sup> Vera Vasylyeva,<sup>b</sup> Klaus Merz<sup>b</sup> and Ulrich Schatzschneider<sup>\*b</sup>

Received 19th August 2009, Accepted 8th December 2009

First published as an Advance Article on the web 22nd January 2010

DOI: 10.1039/b916907e

By combining organometallic groups and peptides, a large number of conjugates with interesting new biological properties can be prepared. Especially, attachment to cell-penetrating peptides (CPP) that act as efficient cell delivery vehicles has come to the fore. However, the presence of the metal moiety in such systems can interfere with standard conjugate synthesis procedures which therefore need to be optimized for every new compound. In this work, we report on the preparation of six new cymantrene-sC18 peptide bioconjugates that were prepared by solid phase peptide synthesis (SPPS) techniques. The cymantrene complexes were chosen for their different linker to the peptide, to study the influence of the linker group on cellular uptake and cell viability of the conjugates. Interestingly, the attachment of the metal complex leads to a non-standard cleavage of the Rink amide linker used in the SPPS protocol under trifluoroacetic acid (TFA) treatment, resulting in peptide amides that are *N*-alkylated at the C-terminus. Furthermore, we found that depending on the type of cymantrene moiety attached, the formation of reactive carbocations which result from decomposition of the resin linker is facilitated and can alkylate the metal complex moiety. Both effects were analyzed by MS/MS studies and cleavage mixtures for efficient elimination of this byproduct formation were identified. Moreover, initial biological testing of the cytotoxicity of one of the bioconjugates gave promising results. Concentration-dependent cell viability studies of Cym1-sC18 on human MCF-7 breast adenocarcinoma cells gave an IC<sub>50</sub> value of 59.8 (± 6.7) μM and demonstrate their potential in anticancer chemotherapy.

## Introduction

In the last few years, a steadily increasing number of systems with exciting new biological activity has been prepared by conjugation of organometallic compounds to bio(macro)molecules.<sup>1–3</sup> In particular, the attachment of metal–organic complexes to peptides is a very promising approach since there exist numerous therapeutically active peptide sequences and their synthesis can easily be achieved by means of solid-phase peptide synthesis (SPPS). Potential applications include use as antitumor<sup>4–6</sup> and antibacterial agents<sup>7,8</sup> as well as radiopharmaceuticals.<sup>9–11</sup> Furthermore, surface-bound ferrocene-peptide conjugates were applied as sensors for proteins.<sup>12</sup>

Metal complex-peptide conjugates can conveniently be prepared by solid-phase peptide synthesis (SPPS). This offers several advantages over solution techniques such as, for instance, the flexible incorporation of the organometallic group at any position

in the amino acid sequence without limitation to terminal sites or side-chain functionalities as in lysines and cysteines. However, the synthesis of metal-peptide conjugates often requires special conditions different from standard SPPS protocols due to the potential sensitivity of the metal functional group and overall conjugate stability. Generally, there are three strategies to prepare metal complex-peptide conjugates:<sup>13</sup> the first one is to synthesize peptide-ligand conjugates followed by complexation with metal ions on a solid support or in solution.<sup>14</sup> The second one is to utilize an organometallic amino acid-like building block during the SPPS chain elongation reaction.<sup>15</sup> Finally, for metal compounds very sensitive towards SPPS conditions, a post-labeling strategy can be used, in which the metal–organic moiety is attached after assembly of the peptide by coupling reactions orthogonal to the peptide side chain functional groups.<sup>16,17</sup>

In this work, we describe the synthesis, characterization, and preliminary study of the biological activity of organometallic peptide conjugates composed of cymantrene carboxylic acids with different linkers between the COOH and cyclopentadienyl groups and sC18, a novel cell-penetrating peptide (CPP).<sup>18</sup> CPPs are delivery vectors for a great variety of different substances and can help to circumvent the problem of limited transport of bioactive molecules into their target cells.<sup>19–22</sup> These peptides are able to internalize without the need of a transporter or receptor molecule and thereby capable of carrying different cargos into cells. We recently reported the successful and efficient delivery

<sup>a</sup>Institut für Biochemie, Universität Leipzig, Brüderstr. 34, D-04103, Leipzig, Germany. E-mail: neundorff@uni-leipzig.de; Fax: (+)49 341 97-36909

<sup>b</sup>Lehrstuhl für Anorganische Chemie I - Bioanorganische Chemie, Ruhr-Universität Bochum NC 3/74, Universitätsstr. 150, D-44801, Bochum, Germany. E-mail: ulrich.schatzschneider@rub.de; Fax: (+)49 234 32-14378

† Electronic supplementary information (ESI) available: Additional experimental details. CCDC reference numbers 681218, 744989, 744990, and 744991. For ESI and crystallographic data in CIF or other electronic format see DOI: 10.1039/b916907e

of nanocrystals, oligonucleotides, and gallium complexes into cancer as well as primary cells using this strategy.<sup>23–25</sup> Cymantrene itself is an easy to functionalize and robust organometallic biomarker which is stable in air and water and has been used for the N-terminal modification of short peptides *via* SPPS.<sup>26</sup> Furthermore, its utility as an IR label of bioactive peptides was demonstrated since the strong C–O stretching vibrations are not obscured by signals from the peptide.<sup>27</sup> However, by attachment to these simple short peptides, no cytotoxic effects on different cancer cell lines could be observed. On the other hand, conjugation of a cymantrene derivative to a more complex CPP based on the peptide hormone human calcitonin (hCT) lead to bioconjugates with promising biological activity. A modified intracellular distribution pattern and significant cytotoxic effects in the low micromolar concentration range were observed on MCF-7 human breast cancer cells while the two constituents themselves were inactive.<sup>28</sup> To further study structure–activity relationships in such a system, we have prepared cymantrene-peptide bioconjugates based on the novel cell-penetrating peptide sC18, which consists of residues 106–121 of the C-terminal region of the cationic antimicrobial peptide cathelicidin (CAP18). This fragment was recently identified as an effective carrier peptide for small organic substances like fluorophors and toxic peptide sequences.<sup>18</sup> In addition, different linkers were introduced between the cymantrene moiety and the peptide to determine their potential influence on cellular uptake and cytotoxicity of the conjugates.

During the evaluation of different SPPS conditions, we identified a number of unexpected byproducts that formed after treatment of the resin with trifluoroacetic acid. Detailed mass spectrometric studies allowed us to rationalize the formation of these species. These results will help to improve the preparation of complex metal-peptide conjugates by solid-phase synthesis methods and provide new insights into the potential reactivity of these cytotoxic compounds.

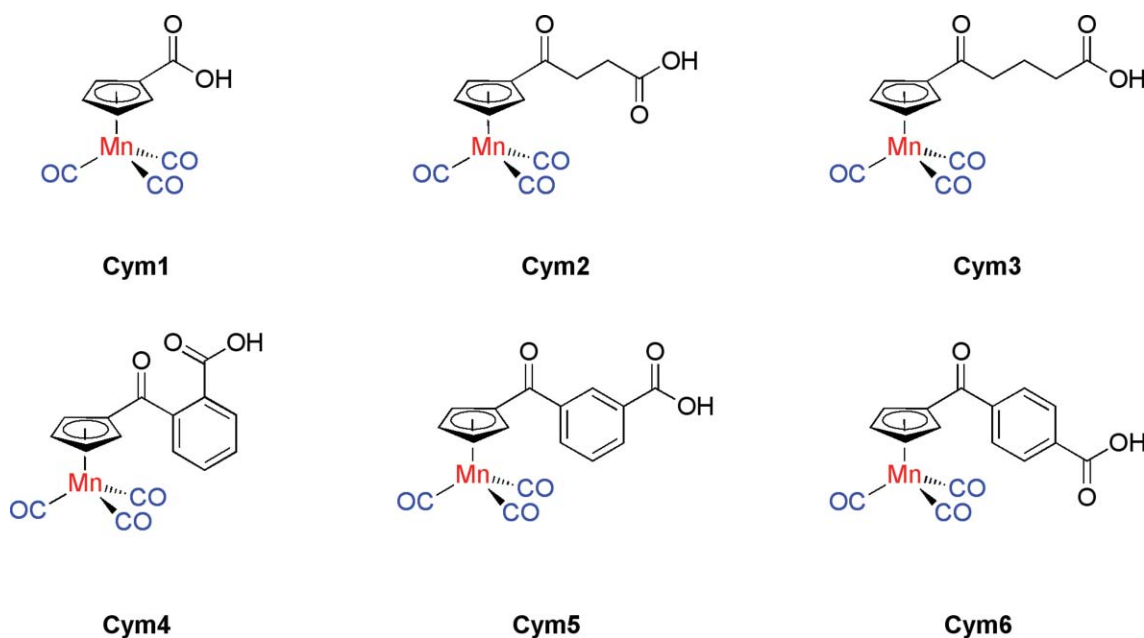
## Results and discussion

### Synthesis of cymantrene carboxylic acids

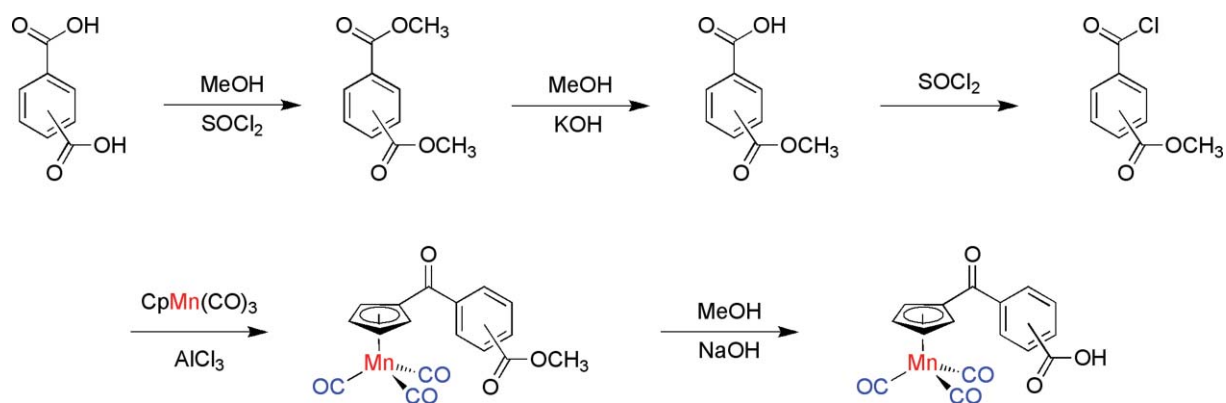
A total of six different cymantrene carboxylic acids **Cym1** to **Cym6** were prepared with different linkers between the cyclopentadienyl ring and the carboxylate group (Scheme 1).

**Cym1** was synthesized by Friedel–Crafts acylation of cymantrene with 2-chlorobenzoyl chloride and subsequent cleavage of the resulting ketone with potassium *tert*-butoxide following the procedure of Biehl and Reeves.<sup>29</sup> Compounds **Cym2** to **Cym4** were also prepared by a Friedel–Crafts reaction of cymantrene with the corresponding cyclic anhydrides in the presence of aluminium chloride as already reported for **Cym2**.<sup>27</sup> The synthesis of **Cym5** and **Cym6**, on the other hand, required the five-step reaction sequence shown in Scheme 2. First, isophthalic or terephthalic acid was converted to the dimethyl ester by treatment with thionylchloride in methanol. Then, one methyl ester group was selectively hydrolyzed by reaction with one equivalent of potassium hydroxide in methanol. The free carboxylic group of the monoester was then converted to the carboxylic acid chloride by heating to reflux in thionylchloride (see ESI†).<sup>30,31</sup> The corresponding acid chloride was reacted with cymantrene in the presence of aluminium chloride to obtain the functionalized half-sandwich complexes in reasonable yield after chromatographic work-up. Finally, the methyl ester was hydrolyzed with sodium hydroxide in methanol to obtain **Cym5** and **Cym6** in good yield and purity.

Single crystals suitable for X-ray structure analysis could be obtained for **Cym3** as well as the three isomeric compounds **Cym4**, **Cym5**, and **Cym6** with either a 1,2-, 1,3- or 1,4-phenylene linker. Relevant parameters are listed in Table 1. The molecular structures are shown in Fig. 1A to 1D, respectively. The metrical parameters of all four compounds (see Table 2) compare well with those recently published for **Cym2** and the crystal packing is also



**Scheme 1** Functionalized cymantrene carboxylic acids **Cym1** to **Cym6** prepared for peptide conjugation.



**Scheme 2** Five-step synthesis of functionalized half-sandwich complexes **Cym5** and **Cym6** by Friedel–Crafts acylation of cymantrene with carboxylic acid chlorides.

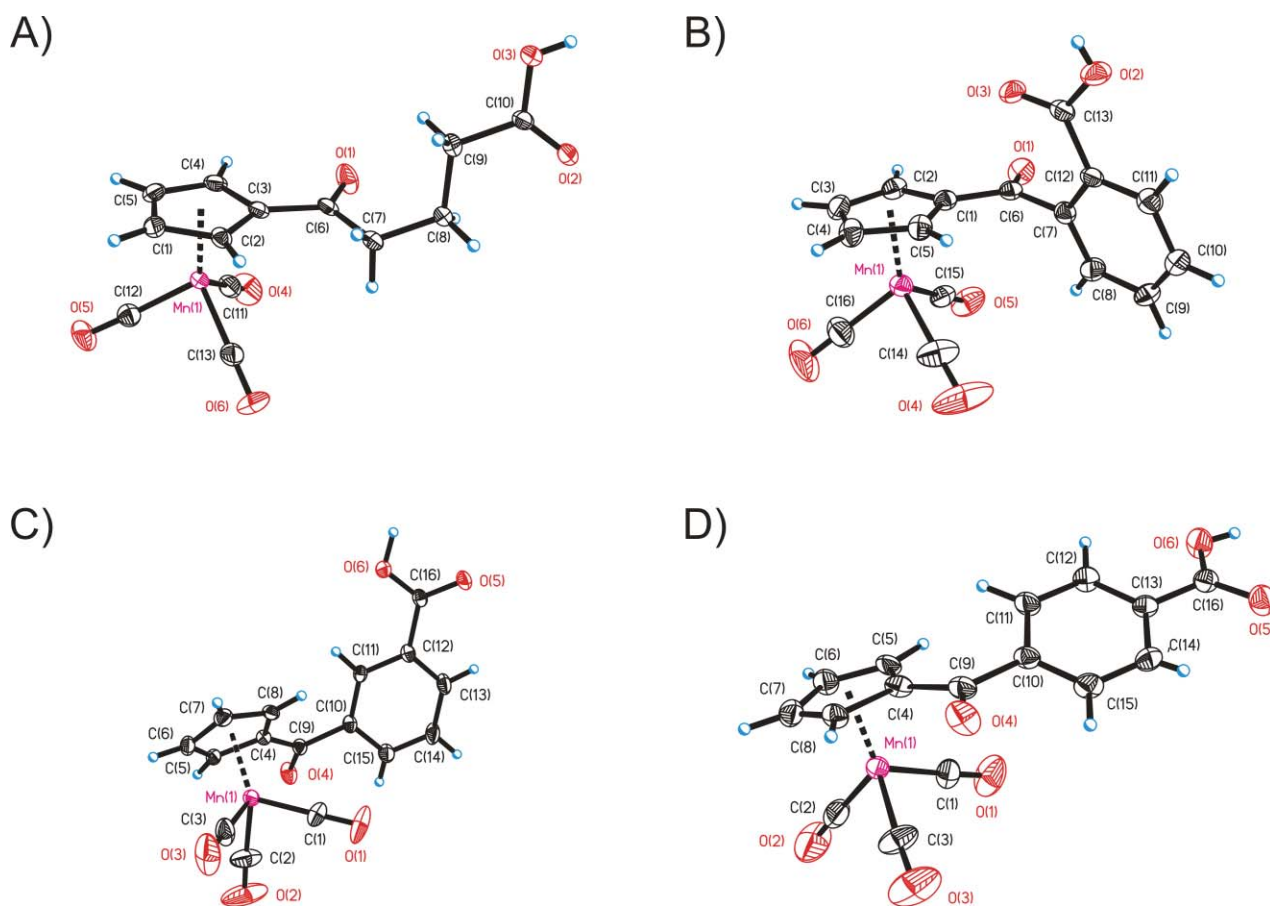


**Fig. 1** Molecular structures of A) **Cym3**, B) **Cym4**, and C) **Cym5**, with ellipsoids drawn at the 50% probability level and D) **Cym6** with ellipsoids drawn at the 30% probability level.

dominated by the formation of hydrogen-bonded dimers *via* the carboxylate groups of two adjacent molecules.<sup>27</sup> The most notable feature is the nearly perpendicular arrangement of the five- and six-membered rings in **Cym4** with a torsion angle of 79.2° to avoid close contacts between the two keto groups and the hydrogen atoms on the carbon centers in *ortho* position to the connecting C=O group. This angle is reduced to 44.3° in **Cym5** and 32.4° in **Cym6**, thus decreasing substantially when going from 1,2- to 1,4-substitution of the phenylene linker. The keto group, on the other hand, remains essentially coplanar with the Cp ring throughout

the series of compounds, with torsion angles in the range of 4.3 to 8.5°.

#### Synthesis of cymantrene-peptide conjugates

Peptides were synthesized on a Rink amide resin according to the Fmoc/*t*Bu-strategy on an automatic peptide synthesizer. After the peptide sequence was assembled, the resin was removed from the synthesizer and the cymantrene carboxylic acids were coupled to the N-terminus of the peptides by standard activation with

**Table 1** Crystallographic parameters for complexes **Cym3** to **Cym6**

Compound	<b>Cym3</b>	<b>Cym4</b>	<b>Cym5</b>	<b>Cym6</b>
Empirical formula	C <sub>13</sub> H <sub>11</sub> MnO <sub>6</sub>	C <sub>16</sub> H <sub>9</sub> MnO <sub>6</sub>	C <sub>16</sub> H <sub>9</sub> MnO <sub>6</sub>	C <sub>16</sub> H <sub>9</sub> MnO <sub>6</sub>
Formula weight	318.16	352.17	352.17	352.17
Dimensions/mm	0.30 × 0.30 × 0.20	0.30 × 0.20 × 0.05	0.20 × 0.20 × 0.10	0.20 × 0.20 × 0.10
Crystal system	Monoclinic	Monoclinic	Monoclinic	Triclinic
Space group	<i>P</i> 2 <sub>1</sub> / <i>c</i>	<i>P</i> 2 <sub>1</sub> / <i>c</i>	<i>P</i> 2 <sub>1</sub> / <i>c</i>	<i>P</i> $\bar{1}$
<i>a</i> /Å	6.435(3)	17.398(8)	11.745(2)	6.3640(12)
<i>b</i> /Å	19.001(9)	7.379(3)	10.670(2)	7.0047(13)
<i>c</i> /Å	10.920(6)	11.634(5)	13.424(3)	18.316(3)
$\alpha$ (°)				90.874(6)
$\beta$ (°)	100.964(9)	103.950(10)	113.63(3)	97.733(5)
$\gamma$ (°)				114.416(4)
<i>V</i> /Å <sup>3</sup>	1310.9(11)	1449.5(11)	1541.1(5)	734.4(2)
<i>Z</i>	4	4	4	2
$\rho_c$ /g cm <sup>-3</sup>	1.612	1.614	1.518	1.593
<i>T</i> /K	213(2)	213(2)	223(2)	223(2)
$\mu$ /mm <sup>-1</sup>	1.029	0.940	0.892	0.927
$\lambda$ /Å (Mo-K $\alpha$ )	0.71073	0.71073	0.71073	0.71073
$2\theta_{\max}$ (°)	25.04	25.04	25.00	24.99
Reflections measured	6915	6822	6722	3092
Unique refl./[ <i>I</i> > 2 $\sigma$ ( <i>I</i> )]	2278/2082	2520/2163	2598/2224	2374/1883
Data completeness	0.982	0.982	0.960	0.917
Variables	186	213	245	209
<i>R</i> [ <i>I</i> > 2 $\sigma$ ( <i>I</i> )]	0.0475	0.0564	0.0556	0.0828
<i>wR</i> [ <i>I</i> > 2 $\sigma$ ( <i>I</i> )]	0.1203	0.1365	0.1409	0.2196
Largest difference map peak/hole in e Å <sup>-3</sup>	0.605/-0.675	0.858/-0.532	0.671/-0.664	0.973/-0.690
Goodness of fit (GOF)	1.134	1.135	1.112	1.019

**Table 2** Selected bond lengths [Å] and angles (°) for **Cym3** to **Cym6**

<b>Cym3</b>	<b>Cym4</b>	<b>Cym5</b>	<b>Cym6</b>
Mn1–C11 1.798(4)	Mn1–C14 1.795(4)	Mn1–C1 1.754(4)	Mn1–C1 1.804(7)
Mn1–C12 1.796(3)	Mn1–C15 1.791(3)	Mn1–C2 1.849(4)	Mn1–C2 1.800(9)
Mn1–C13 1.800(4)	Mn1–C16 1.791(4)	Mn1–C3 1.835(4)	Mn1–C3 1.795(8)
C11–O4 1.142(4)	C14–O4 1.142(4)	C1–O1 1.120(5)	C1–O1 1.149(8)
C12–O5 1.144(4)	C15–O5 1.143(4)	C2–O2 1.179(6)	C2–O2 1.163(10)
C13–O6 1.142(4)	C16–O6 1.143(5)	C3–O3 1.161(5)	C3–O3 1.145(9)
Mn1–C1 2.148(3)	Mn1–C1 2.121(3)	Mn1–C4 2.196(3)	Mn1–C4 2.149(8)
Mn1–C2 2.143(3)	Mn1–C2 2.146(3)	Mn1–C5 2.180(3)	Mn1–C5 2.167(7)
Mn1–C3 2.129(3)	Mn1–C3 2.158(3)	Mn1–C6 2.135(3)	Mn1–C6 2.166(7)
Mn1–C4 2.134(3)	Mn1–C4 2.152(3)	Mn1–C7 2.178(3)	Mn1–C7 2.186(8)
Mn1–C5 2.139(3)	Mn1–C5 2.130(3)	Mn1–C8 2.227(3)	Mn1–C8 2.158(7)
C6–O1 1.220(4)	C6–O1 1.216(3)	C16–O5 1.255(4)	C9–O4 1.225(8)
C10–O2 1.217(4)	C13–O3 1.228(4)	C16–O6 1.256(4)	C16–O5 1.289(8)
C10–O3 1.310(4)	C13–O2 1.304(4)	C9–O4 1.264(4)	C16–O6 1.275(8)
C11–Mn1–C12 91.83(15)	C14–Mn1–C15 91.33(16)	C1–Mn1–C2 90.8(2)	C1–Mn1–C2 91.3(3)
C11–Mn1–C13 92.97(16)	C14–Mn1–C16 91.1(2)	C1–Mn1–C3 89.45(18)	C1–Mn1–C3 91.5(4)
C12–Mn1–C13 92.26(15)	C15–Mn1–C16 90.68(16)	C2–Mn1–C3 92.3(3)	C2–Mn1–C3 91.6(4)

1-hydroxybenzotriazole (HOBt) and *N,N*-diisopropylcarbodiimide (DIC). Subsequently, the bioconjugates were cleaved from the resin with a mixture of 95% TFA, 2.5% triisopropylsilane (TIS) and 2.5% water. Unexpectedly, additional peptide conjugates with a molecular weight increased by 106 Da relative to that of the desired compounds were also detected in high abundance (~60% of total product) in the MALDI and ESI mass spectra. Recently, such side products were also reported by Stathopoulos *et al.* and identified as a resin-, cleavage mixture-, and sequence-dependent problem.<sup>32</sup> The authors suggested that the molecular weight increase by 106 Da results from the alternative cleavage of the Rink amide linker in the position 1 indicated in Fig. 2, leading to the formation of

C-terminally *N*-alkylated peptide amides. Interestingly, in our case, this side-product formation seems to be dependent on the cymantrene group attached to the peptide since we observed no byproducts during the synthesis of the parent peptide sC18.<sup>18</sup> However, we found that this sequence-dependent modification could be suppressed by using a cleavage mixture containing 1,3-dimethoxybenzene (1,3-DMB), a substance that is reported to prevent the linker decomposition during peptide cleavage.<sup>32</sup>

Therefore, cleavage of the cymantrene-peptide bioconjugates from the resin was repeated using a mixture of 95% TFA and 5% 1,3-DMB, leading to the successful isolation of the **Cym1**-, **Cym2**- and **Cym3-sC18** derivatives. Typical MALDI mass spectra and HPLC traces for **Cym1-sC18** are shown in Fig. 3. As demonstrated

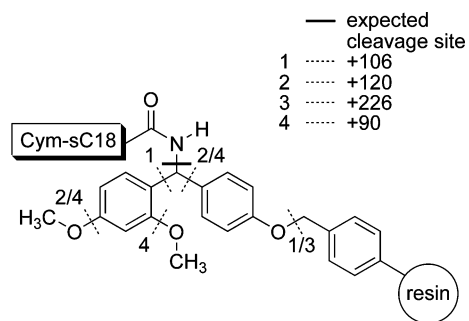


**Fig. 2** Possible cleavage sites of the Rink amide linker giving rise to the molecular weight increase determined for the byproducts.

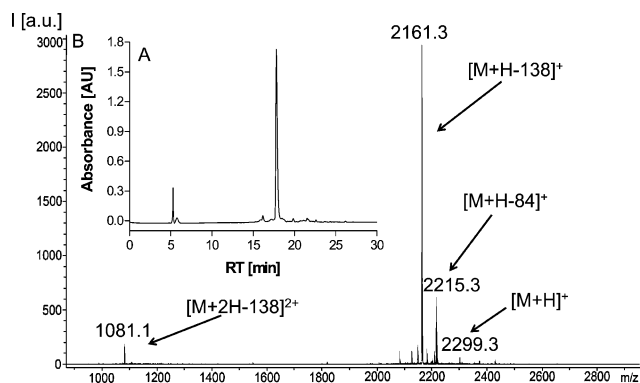


**Fig. 3** Typical analytical data for **Cym1-sC18**: (A) HPLC chromatogram obtained with a gradient of 10 to 60% acetonitrile–water over 30 min. (B) MALDI-MS spectrum of the compound. The peak at a retention time of ~5 min in the HPLC chromatogram is the injection peak.

in particular by the HPLC trace in Fig. 3A, the metal complex-peptide conjugates were obtained in good purity.

In the MALDI-MS analysis of the products, the most intense signal was identified as  $[M + H - \text{Mn}(\text{CO})_3]^+$ , indicating the loss of the metal tricarbonyl moiety under MALDI conditions (Fig. 3B). Also, the  $[M + H]^+$  and  $[M + H - (\text{CO})_3]^+$  peaks were detected. Recently, this phenomenon was also observed for other cymantrene-peptide bioconjugates.<sup>28</sup> However, ESI-MS showed only the  $[M + 5H]^{5+}$  and  $[M + 6H]^{6+}$  signals of the intact products (see Table 3).

Surprisingly, cleavage of **Cym4-sC18** incorporating a 1,2-phenylene linker with 1,3-DMB as the scavenger still did not yield the expected target molecule since mainly a product with a molecular weight of 120 Da higher than calculated for **Cym4-sC18** was isolated in nearly 90% yield. Furthermore, we detected additional byproducts at +90 and +226 Da compared to the desired compound. As shown in Fig. 2, decomposition of the Rink amide linker is also possible at the positions labeled as 4, 2, and 3, thus leading to the formation of *N*-alkylated peptide amides with a molecular weight increased by 90, 120, and 226 Da, respectively. Recently, we reported on the successful synthesis and biological characterisation of Cym4-hCT(18–32)-k7, a cymantrene-peptide bioconjugate where the metal-containing fragment was coupled to a branched CPP.<sup>28</sup> During the synthesis of this conjugate, no byproducts resulting from the decomposition of the Rink amide resin were observed. In addition, we did not observe byproducts with a molecular weight increased by 120 Da after coupling of **Cym1**, **Cym2**, or **Cym3** to the sC18-peptide. Moreover,

successful coupling of **Cym2** to different short carrier peptides has been described.<sup>27</sup> In summary, all these findings suggest two different effects: first, decomposition of the Rink amide linker is not only dependent on the peptide sequence, as described by Stathopoulos *et al.*, but also on the modification of the peptide with the organometallic complex. In addition, it also seems to depend on the cymantrene carboxylic acid attached, resulting in alkylation of the metal complex itself, most likely at the aromatic linker. To suppress the formation of those byproducts, several different cleavage cocktails were tested containing either 1,3-DMB, methanol, 2-methylanisole (2-MA), or 4-methylanisole (4-MA). All these compounds are related to the carbocations that might form during cleavage of the resin linker. In Table 4, the results of the analysis of the resulting products with MALDI- and ESI-MS as well as analytical RP-HPLC are collected.

Interestingly, mixtures I, II, III, VII, IX, and X yielded the [**Cym4-sC18** + 106] byproduct and all mixtures except for I and II also gave the [**Cym4-sC18** + 120] compound. Only when using mixtures V, VII, VIII, XI, and XII (highlighted in bold in Table 4) was the desired target molecule formed in significant yield, as shown by ESI- and MALDI-MS analysis. Variation of the incubation time did not lead to considerable differences (data not shown). However, it was still not possible to completely eliminate the byproduct formation and only with cleavage mixture XII could the product be obtained in relatively high yield (~70%). It was purified by preparative HPLC and finally isolated in very high purity (>99%).

It is interesting to note that during the synthesis of the **Cym5**- and **Cym6**-peptide bioconjugates under the same conditions as employed for the **Cym4-sC18** conjugate, we did not observe any byproducts at a molecular mass higher by 120, nor when using a cleavage mixture containing TFA/water (95/5% v/v) nor by the use of TFA/1,3-DMB (95/5% v/v). This is an additional hint that the +120 Da byproduct formation depends on the linker of the metal complex attached to the peptide.

### Structural characterization of the byproducts by MS/MS studies

Our results suggest that during cymantrene-peptide synthesis, two different side reactions occur. On the one hand, non-standard cleavage of the Rink amide linker leads to the formation of C-terminally *N*-alkylated peptide amide byproducts and on the other hand, alkylation of the aromatic phenylene linker between the cymantrene moiety and the peptide by carbocations resulting from decomposition of the resin linker occurs. We hypothesized that in the former case, cleavage of the Rink amide linker at position 1 (see Fig. 2) favors the liberation of the peptide from the resin without formation of an intermediate carbocation. In contrast, the byproduct with +120 Da must result from the formation of a carbocation that can react with the **Cym4** moiety, most likely at the 1,2-phenylene linker. To gather evidence to prove this hypothesis, we carried out additional MS/MS studies in which the precursor ions of the +120 Da byproducts were mass-selected and fragmented (Fig. 4).

The *x*, *y*, and *z* as well as the corresponding *a*, *b*, and *c* series were observed, pointing to a distribution of cleavage sites as shown in Fig. 4A. The cymantrene-bearing fragments yielded either the expected mass peak or those corresponding to a loss of the three carbonyls or the whole  $\text{Mn}(\text{CO})_3$  group. Interestingly, the *x*, *y*, and

**Table 3** Analytical data of the cymantrene peptide bioconjugates **Cym1-** to **Cym6-sC18**

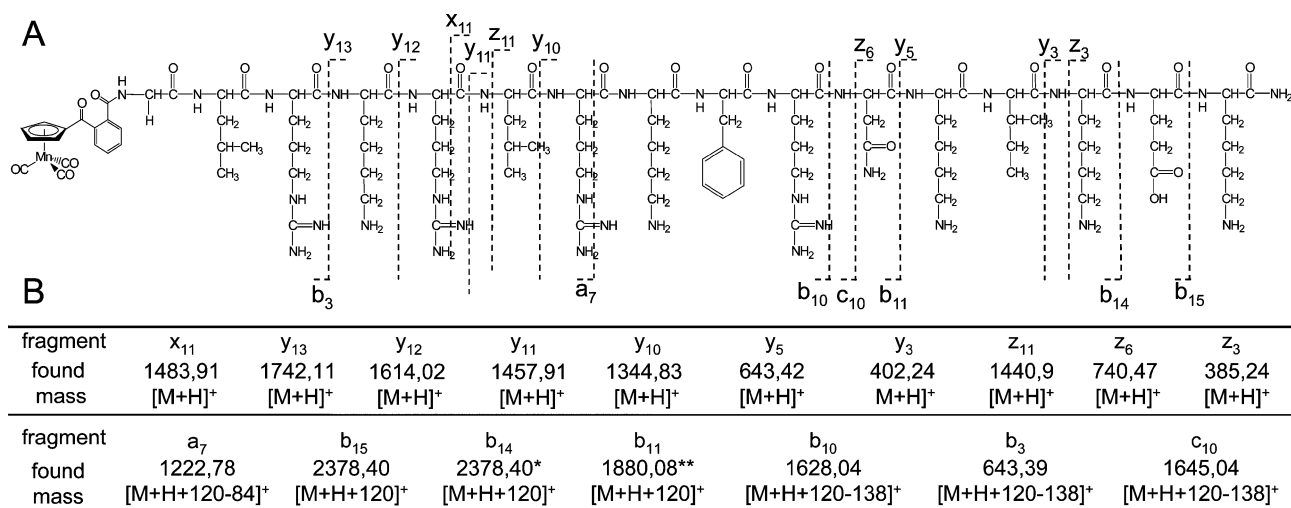
Peptide	Sequence <sup>a</sup>	MW <sub>calc.</sub>	MALDI <sub>exp.</sub>	ESI <sub>calc.</sub>	ESI <sub>exp.</sub>
<b>Cym1-sC18</b>	Cym1-GLRKRLRKFRNKIKEK	2298.4	2299.3 [M + H] <sup>+</sup>	460.7 [M + 5H] <sup>5+</sup>	460.8 [M + 5H] <sup>5+</sup>
<b>Cym2-sC18</b>	Cym2-GLRKRLRKFRNKIKEK	2354.5	2355.5 [M + H] <sup>+</sup>	471.9 [M + 5H] <sup>5+</sup>	472.0 [M + 5H] <sup>5+</sup>
<b>Cym3-sC18</b>	Cym3-GLRKRLRKFRNKIKEK	2368.5	2369.3 [M + H] <sup>+</sup>	474.7 [M + 5H] <sup>5+</sup>	474.9 [M + 5H] <sup>5+</sup>
<b>Cym4-sC18</b>	Cym4-GLRKRLRKFRNKIKEK	2402.5	2403.4 [M + H] <sup>+</sup>	481.5 [M + 5H] <sup>5+</sup>	481.7 [M + 5H] <sup>5+</sup>
<b>Cym5-sC18</b>	Cym5-GLRKRLRKFRNKIKEK	2402.5	2403.4 [M + H] <sup>+</sup>	481.5 [M + 5H] <sup>5+</sup>	481.7 [M + 5H] <sup>5+</sup>
<b>Cym6-sC18</b>	Cym6-GLRKRLRKFRNKIKEK	2402.5	2403.4 [M + H] <sup>+</sup>	481.5 [M + 5H] <sup>5+</sup>	481.7 [M + 5H] <sup>5+</sup>

<sup>a</sup> All peptides are C-terminally amidated.

**Table 4** Different scavenger mixtures tested for cleavage of **Cym4-sC18**

No.	Reagent mixture <sup>a</sup>	Ratio	Product [%]	[M + 106] <sup>+</sup> [%]	[M + 120] <sup>+</sup> [%]	Other byproducts [%]
I	TFA : TA : TK	90 : 5 : 5	—	< 95	—	> 5
II	TFA : TA : EDT	90 : 7 : 3	—	< 10	—	> 90
III	TFA : H <sub>2</sub> O : TIS	95 : 2.5 : 2.5	—	< 15	< 15	> 70
IV	TFA : DMB	95 : 5	—	—	< 90	> 10
V	<b>TFA : TIS : EDT : H<sub>2</sub>O</b>	<b>94 : 1 : 2.5 : 2.5</b>	<b>&lt; 60</b>	—	< 30	> 10
VI	TFA : DMB : TIS	92.5 : 5 : 2.5	—	—	< 90	> 10
VII	<b>TFA : anisol : H<sub>2</sub>O : phenol</b>	<b>85 : 5 : 5 : 5</b>	<b>&lt; 5</b>	< 5	< 60	> 30
VIII	<b>TFA : H<sub>2</sub>O : MeOH</b>	<b>90 : 5 : 5</b>	<b>&lt; 65</b>	—	< 25	> 10
IX	TFA : 2-MA : 4-MA	95 : 2.5 : 2.5	—	< 5	< 55	> 40
X	TFA : 2-MA	95 : 5	—	< 10	< 40	> 50
XI	<b>TFA : 4-MA</b>	<b>95 : 5</b>	<b>&lt; 20</b>	—	< 50	> 30
XII	<b>TFA : H<sub>2</sub>O</b>	<b>95 : 5</b>	<b>&lt; 70</b>	—	< 25	> 5

<sup>a</sup> **Bold:** product was obtained besides byproducts. TFA: trifluoroacetic acid, TA: thioanisol, TK: thiocresol, EDT: 1,2-ethanedithiol, TIS: triisopropylsilane, DMB: 1,3-dimethoxybenzene, 2-/4-MA: 2- or 4-methylanisol.



\*also the [M+H+120-84]<sup>+</sup> peak was observed; \*\*also the [M+H+120-84]<sup>+</sup> peak and the [M+H+120-138]<sup>+</sup> peak were observed

**Fig. 4** (A) Fragmentation pattern of [**Cym4-sC18** + 120] and (B) experimental masses of the different fragments detected by MS/MS.

z series of the byproduct [**Cym4-sC18** + 120] showed fragments with the expected molecular weight whereas the a, b, and c series had a mass increased by 120 Da. These results further support the idea that the [**Cym4-sC18** + 120] byproduct results from an alkylation at the aromatic phenylene linker of the cymantrene complex. We also analyzed the [**Cym3-sC18** + 106] byproduct (data not shown) in which the x, y, and z series showed an increase of molecular weight by 106 Da as expected while the a, b, and c series yielded the expected mass providing additional support that, in this case, the [**Cym3-sC18** + 106] byproduct results from

cleavage of the resin at position 1 as depicted in Fig. 2. This assumption is further supported by the synthesis of a cymantrene-peptide conjugate that was modified with two Cym4 units (data not shown). After cleavage from the solid support with 95% TFA and 5% 1,3-DMB, we observed peaks in the MALDI and ESI mass spectra with a molecular weight increased by 240 Da. This is consistent with a modification on both cymantrene units by groups with a mass of 120 Da each and confirms the assumption that the modification takes place at the phenylene linker. The fact that both of the substituents of the phenyl ring are electron-withdrawing

could explain the preferential attack of the carbocation in the *meta* position. As outlined in Fig. 5, reaction at the 1,2-substituted phenylene ring should be favored due to the fact that it has two, the 1,3-substituted phenylene ring only one and the 1,4-substituted phenylene ring no, positions prone to attack by the carbocation.

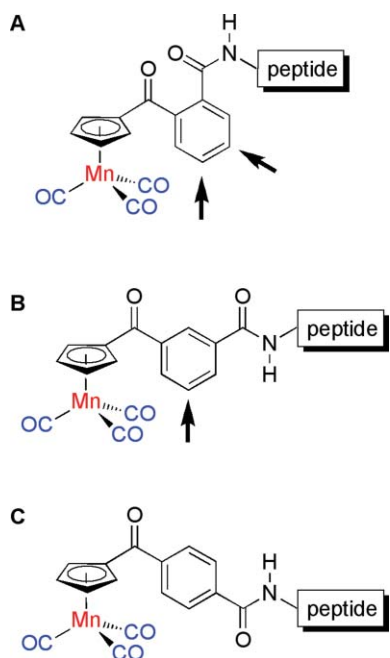


**Fig. 5** Potential positions for the attack of reactive carbocations on the linker in A) **Cym4-**, B) **Cym5-**, and C) **Cym6-sC18** leading to byproducts with a mass increased by 120 Da as indicated by arrows.

### Preliminary tests of biological activity

For a preliminary study of the biological activity, we selected bioconjugate **Cym1-sC18** and tested it on the human breast adenocarcinoma cancer cell line MCF-7. The results of the resazurin-based cell viability test are shown in Fig. 6. After incubation of the cells for 24 h with the **sC18** peptide or the cymantrene carboxylic acid **Cym1** alone, no effect could be observed. This is in line with other recent results on both the **sC18** peptide itself as well as other cymantrene bioconjugates, in which both the peptide and the organometallic group itself were found to be inactive.<sup>26–28</sup> In contrast, incubation of MCF-7 cells with the cymantrene-peptide bioconjugate **Cym1-sC18** resulted in a clear concentration-dependent decrease of the cell viability. From non-linear curve fitting, an  $IC_{50}$  value of  $(59.8 \pm 6.7) \mu\text{M}$  was determined for this compound. While other cymantrene-peptide conjugates with CPPs like Tat and other sequences had no effect on the human colon carcinoma cell line HT-29 in the concentration range tested ( $<100 \mu\text{M}$ ), a more complex **Cym4-hCT(18–32)-k7** conjugate exhibited an  $IC_{50}$  of about  $30 \mu\text{M}$  on MCF-7 cells.<sup>28</sup> These results suggest that the biological activity depends on both the cell line as well as the carrier peptide used. In particular, our model conjugate investigated in this work shows promising activity and a detailed study of the biological activity of all peptide conjugates presented here will be the subject of an upcoming study from our labs.

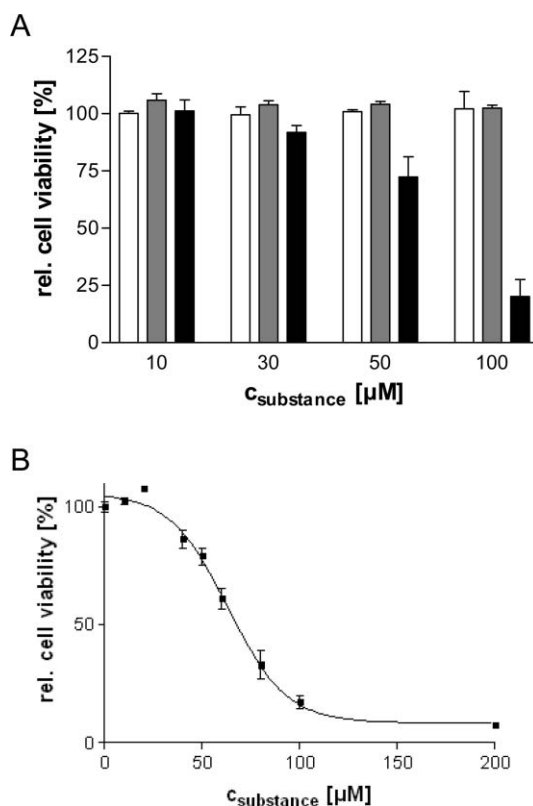


**Fig. 6** (A) Relative cell viability of MCF-7 cells determined with the resazurin assay after treatment for 24 h with **sC18** (white), **Cym1** (grey), and **Cym1-sC18** (black). (B)  $IC_{50}$  curve of **Cym1-sC18**. Data are normalized to untreated cells (100% viability), for the control samples, cells were treated with ethanol (70%). All experiments were done with  $n$  (number of experiments)  $\geq 2$  in triplicate.

### Conclusion

In this work, six new functionalized cymantrenes were prepared and conjugated by SPPS to the novel **sC18** carrier peptide, which is made up of residues 106–121 of the C-terminal region of the cationic antimicrobial peptide cathelicidin (CAP18). Four of the cymantrenes were additionally characterized by X-ray structure determination. In the peptide functionalization step, we found that decomposition of the Rink amide linker can lead, on one hand, to the formation of C-terminally *N*-alkylated amide byproducts and on the other hand, to the formation of reactive carbocations which undergo further reactions with the aromatic linker of the attached metal complex. Occurrence of both processes depends on the peptide sequence as well as the metal complex attached. The non-standard Rink amide linker cleavage could be suppressed by addition of 1,3-dimethoxybenzene (1,3-DMB) to the cleavage mixture while formation of the carbocation could be reduced by use of a combination of trifluoroacetic acid (TFA) and water. Preliminary testing of the biological activity of the **Cym1-sC18** bioconjugate on human MCF-7 breast cancer cells demonstrated the utility of the combination of a functionalized cymantrene group with the **sC18** carrier peptide to generate organometallic peptide conjugates with promising anticancer activity. Further studies will be aimed at clarifying the uptake mechanism, internalization pattern and biological activity of all six cymantrene-CPP bioconjugates presented here.

## Experimental

### General procedures

Reactions were carried out in oven-dried Schlenk glassware under an atmosphere of pure dinitrogen when necessary. Solvents were dried over molecular sieves and degassed prior to use. Fmoc amino acid derivatives were purchased from Iris Biotech GmbH, CBL, and Novabiochem. 1-Hydroxybenzotriazole (HOBt) and 4-(2',4'-dimethoxyphenyl-Fmoc-aminomethyl)-phenoxy-methyl-linked polystyrene (Rink amide) were obtained from Novabiochem. 1,2-Ethanedithiol (EDT), thioanisole (TA), thiocresol (TK), piperidine, and triisopropylsilane (TIS) were purchased from Fluka. Dichloromethane (DCM) and *N,N*-dimethylformamide (DMF) were Biosolve products and 2-methylanisole (2-MA) and 4-methylanisole (4-MA) from Acros. *N,N*-diisopropylcarbodiimide (DIC) was obtained from Iris Biotech GmbH, anisole, trifluoroacetic acid (TFA), and 1,3-dimethoxybenzene (DMB) from Sigma-Aldrich. Phenol was purchased from Riedel-de Haen and gradient degree high-performance liquid chromatography (HPLC) solvents acetonitrile (ACN) from Chromanorm and methanol from LiChrosolv. All other chemicals were obtained from commercial sources and used without further purification. NMR spectra were recorded on Bruker DPX 200, DPX 250, or DRX 400 spectrometers ( $^1\text{H}$  at 200.13 and 400.13 MHz, respectively;  $^{13}\text{C}$  at 50.33, 62.90 and 100.62 MHz). Chemical shifts  $\delta$  in ppm indicate a downfield shift relative to tetramethylsilane (TMS) and were referenced relative to the signal of the solvent.<sup>33</sup> Coupling constants  $J$  are given in Hz. Individual peaks are marked as singlet (s), doublet (d), triplet (t) quartet (q), or multiplet (m). Mass spectra of small molecules were measured on Bruker Esquire 6000 (ESI) and VG Autospec (EI, FAB) instruments, only characteristic fragments are given for the most abundant isotope peak. The solvent flow rate for the ESI measurements was  $4\ \mu\text{l}\ \text{min}^{-1}$  with a nebulizer pressure of 10 psi and a dry gas flow rate of  $5\ \text{l}\ \text{min}^{-1}$  at a dry gas temperature of  $300\ ^\circ\text{C}$ . IR spectra were recorded on pure solid samples with a Bruker Tensor 27 IR spectrometer equipped with a Pike MIRacle Micro ATR accessory. The elemental composition of the compounds was determined with a VarioEL analyzer from Elementar Analysensysteme GmbH.

### Synthesis of cymantrene keto carboxylic acids

The three-step synthesis of the terephthalic and isophthalic acid monomethyl ester chlorides **4** and **8** used in the Friedel–Crafts acylations is described in the ESI.†

### Preparation of Cym5 methyl ester

Aluminium chloride (333.8 mg, 2.5 mmol, Fluka,  $\geq 99.0\%$ ) and anhydrous dichloromethane (20 ml) were placed in a 50 ml three-necked Schlenk-flask equipped with a reflux condenser and internal thermometer. The solution was cooled to  $0$  to  $5\ ^\circ\text{C}$  with ice while stirring. Then, solid **4** (243.3 mg, 1.23 mmol) was added in small portions followed by cymantrene (250 mg, 1.23 mmol) while the temperature was maintained at  $0$  to  $5\ ^\circ\text{C}$ . After 1 h, the reaction mixture was allowed to warm to room temperature and stirring continued overnight. The reaction mixture was then poured into a mixture of ice/water (100 ml) and concentrated hydrochloric

acid (10 ml). The layers were separated and the aqueous phase extracted with dichloromethane ( $3 \times 50\ \text{ml}$ ). The combined organic phases were then washed with water and saturated aqueous sodium carbonate solution. The solvent was removed from the organic phase and the residue purified by column chromatography on silica using a mixture of *n*-hexane–ethyl acetate 5 : 3 (v/v) as the eluent ( $R_f$  0.60). Yield: 54%.  $^1\text{H-NMR}$  (200 MHz,  $(\text{CD}_3)_2\text{CO}$ ,  $\delta_{\text{ppm}}$ ): 8.43 (s, 1H,  $\text{H}_{\text{Ar}}$ ), 8.25 (d, 1H,  $^3J = 7.8\ \text{Hz}$ ,  $\text{H}_{\text{Ar}}$ ), 8.09 (d, 1H,  $^3J = 7.8\ \text{Hz}$ ,  $\text{H}_{\text{Ar}}$ ), 7.72 (t, 1H,  $^3J = 7.7\ \text{Hz}$ ,  $\text{H}_{\text{Ar}}$ ), 5.74 (s, 2H, Cp), 5.26 (s, 2H, Cp), 3.93 (s, 3H,  $-\text{OCH}_3$ );  $^{13}\text{C-NMR}$  (62.9 MHz,  $\text{CDCl}_3$ ,  $\delta_{\text{ppm}}$ ): 222.76 (C=O), 191.38 (C=O), 166.14 (C=O), 138.05 ( $\text{C}_{\text{Ar}}$ ), 133.64 ( $\text{C}_{\text{Ar}}$ ), 132.26 ( $\text{CH}_{\text{Ar}}$ ), 131.22 ( $\text{CH}_{\text{Ar}}$ ), 130.46 ( $\text{CH}_{\text{Ar}}$ ), 127.91 ( $\text{CH}_{\text{Ar}}$ ), 97.98 (Cp), 91.18 (Cp), 89.69 (Cp), 86.46 (Cp), 82.72 (Cp), 53.72 ( $-\text{OCH}_3$ ); FAB-MS:  $m/z = 367.0\ [\text{M} + \text{H}]^+$ ; IR (ATR,  $\text{cm}^{-1}$ ): 2019, 1919, 1715, 1641, 1271, 1163; Elemental analysis (%): calc. for  $\text{C}_{17}\text{H}_{11}\text{MnO}_6$ : C 55.76, H 3.03 found: C 55.39, H 2.61.

The **Cym6 methyl ester** was prepared by a similar procedure using **8** instead of **4** and with a slightly different chromatographic work-up. For this compound, *n*-hexane–ethyl acetate 5 : 2 (v/v) was used as the eluent ( $R_f$  0.45) to give the product as a yellow solid. Yield: 45%.  $^1\text{H-NMR}$  (400 MHz,  $\text{CDCl}_3$ ,  $\delta_{\text{ppm}}$ ): 8.16 (d, 2H,  $^3J = 8.0\ \text{Hz}$ ,  $\text{H}_{\text{Ar}}$ ), 7.82 (d, 2H,  $^3J = 8.0\ \text{Hz}$ ,  $\text{H}_{\text{Ar}}$ ), 5.49 (s, 2H, Cp), 4.93 (s, 2H, Cp), 3.96 (s, 3H,  $-\text{OCH}_3$ );  $^{13}\text{C-NMR}$  (100.6 MHz,  $\text{CDCl}_3$ ,  $\delta_{\text{ppm}}$ ): 222.72 (C=O), 191.89 (C=O), 166.22 (C=O), 141.65 ( $\text{C}_{\text{Ar}}$ ), 133.53 ( $\text{C}_{\text{Ar}}$ ), 129.97 ( $\text{CH}_{\text{Ar}}$ ), 127.98 ( $\text{CH}_{\text{Ar}}$ ), 91.15 (Cp), 88.30 (Cp), 84.19 (Cp), 52.63 ( $-\text{OCH}_3$ ); FAB-MS:  $m/z = 367.0\ [\text{M} + \text{H}]^+$ ; IR (ATR,  $\text{cm}^{-1}$ ): 2020.12, 1962.93, 1921.38, 1721.82, 1643.55, 1278.93, 1112.89; Elemental analysis (%): calc. for  $\text{C}_{17}\text{H}_{11}\text{MnO}_6$ : C 55.76, H 3.03, found: C 55.13, H 3.21.

**Cym5 and Cym6.** An aqueous solution of sodium hydroxide (1 M, 10 ml) was added to **Cym5** or **Cym6 methyl ester** (200 mg, 0.55 mmol) in methanol (50 ml) and stirred at room temperature. The reaction was monitored with TLC (silica, *n*-hexane–ethyl acetate 5 : 2 v/v) until the disappearance of the starting material was complete. Then, the solvent was removed and water (200 ml) added to the residue. The solution was washed with dichloromethane ( $3 \times 50\ \text{ml}$ ), and acidified with concentrated hydrochloric acid to pH 1. The precipitate was taken up in ethyl acetate and dried over magnesium sulfate. After removal of the solvent, **Cym5** and **Cym6** were obtained as yellow solids. Yields: 85% for both compounds.

**Cym5.**  $^1\text{H-NMR}$  (200 MHz,  $\text{CD}_3\text{OD}$ ,  $\delta_{\text{ppm}}$ ): 8.28 (s, 2H,  $\text{H}_{\text{Ar}}$ ), 7.94 (s, 1H,  $\text{H}_{\text{Ar}}$ ), 7.66 (s, 1H,  $\text{H}_{\text{Ar}}$ ), 5.66 (s, 2H, Cp), 5.14 (s, 2H, Cp);  $^{13}\text{C-NMR}$  (62.9 MHz,  $(\text{CD}_3)_2\text{SO}$ ,  $\delta_{\text{ppm}}$ ): 224.33 (C=O), 191.79 (C=O), 170.35 (C=O), 139.28 ( $\text{C}_{\text{Ar}}$ ), 134.58 ( $\text{C}_{\text{Ar}}$ ), 132.02 ( $\text{CH}_{\text{Ar}}$ ), 131.34 ( $\text{CH}_{\text{Ar}}$ ), 130.30 ( $\text{CH}_{\text{Ar}}$ ), 128.73 ( $\text{CH}_{\text{Ar}}$ ), 97.20 (Cp), 92.69 (Cp), 91.12 (Cp); ESI-MS (negative):  $m/z = 351.0\ [\text{M} - \text{H}]^-$ ; IR (ATR,  $\text{cm}^{-1}$ ): 2557, 2024, 1945, 1692, 1649, 1307, 1265; Elemental analysis (%): calc. for  $\text{C}_{16}\text{H}_9\text{MnO}_6$ : C 54.57, H 2.58, found: C 54.24, H 2.60.

**Cym6.**  $^1\text{H-NMR}$  (200 MHz,  $(\text{CD}_3)_2\text{CO}$ ,  $\delta_{\text{ppm}}$ ): 8.19 (s, 2H,  $\text{H}_{\text{Ar}}$ ), 7.94 (s, 2H,  $\text{H}_{\text{Ar}}$ ), 5.76 (s, 2H, Cp), 5.25 (s, 2H, Cp);  $^{13}\text{C-NMR}$  (62.9 MHz,  $(\text{CD}_3)_2\text{SO}$ ,  $\delta_{\text{ppm}}$ ): 223.44 (C=O), 191.21 (C=O), 166.21 (C=O), 140.47 ( $\text{C}_{\text{Ar}}$ ), 133.96 ( $\text{CH}_{\text{Ar}}$ ), 90.94 (Cp), 89.20 (Cp), 85.81 (Cp) 85.13 (Cp); ESI-MS(negative):  $m/z = 350.9\ [\text{M} - \text{H}]^-$ ; IR (ATR,  $\text{cm}^{-1}$ ): 2543, 2028, 1928, 1683, 1632, 1378, 1285; Elemental analysis (%): calc. for  $\text{C}_{16}\text{H}_9\text{MnO}_6$ : C 54.57, H 2.58, found: C 54.69, H 3.02.

## Synthesis of cymantrene-peptide conjugates

sC18 was synthesized by automated solid-phase peptide synthesis (SPPS) on a Rink amide resin (30 mg, resin loading 0.45 mmol g<sup>-1</sup>) using the Fmoc/*t*Bu-strategy on a multiple synthesizer (Syro, MultiSynTech, Bochum, Germany) as described elsewhere.<sup>34</sup> Manual coupling of cymantrene acids **Cym1** to **Cym6** to the N-terminus was achieved by activation with 5 eq. HOBt/DIC. Peptides were cleaved from the resin with TFA under addition of different scavenger mixtures (see Table 4) for 1 to 3 h and precipitated by addition of ice-cold diethylether. The compounds were analyzed by reversed-phase (RP) HPLC, matrix-assisted laser desorption ionization time of flight (MALDI-ToF) mass spectrometry (MS) and electrospray ionization (ESI) MS. ESI ion trap measurements were performed on a Bruker HCT mass spectrometer. MALDI-ToF mass spectrometry was carried out on a Bruker Daltonics Ultraflex III instrument in reflection mode. Analytical RP-HPLC was done on a Merck-Hitachi system with a Grace Vydac 218TP54 column (4.6 × 250 mm; 5 μm; 300 Å) using a linear gradient of 10 to 60% of acetonitrile/0.08% TFA in water/0.1% TFA over 30 min and a flow rate of 0.6 ml min<sup>-1</sup> or a linear gradient of 40 to 90% of methanol/0.08% TFA in water/0.1% TFA over 30 min at the same flow rate. The functionalized peptides were purified by semi-preparative or preparative RP-HPLC on a Shimadzu Chromatopac system using the same binary elution system as used in the analytical HPLC. In the first case, a Vydac 218TP510 C18 column (250 × 4.6 mm; 5 μm; 300 Å) with a linear gradient running from 20 to 60% water/0.1% TFA in acetonitrile/0.08% TFA over 50 min or from 40 to 80% water/0.1% TFA in acetonitrile/0.08% TFA over 50 min was used. Preparative HPLC was carried out utilizing a Vydac 218TP1022 C18 column (250 × 20 mm; 10 μm; 300 Å) and the same linear gradients as described above. Fractions containing peptide conjugates were collected and analyzed by analytical HPLC and MALDI-ToF MS. Pure fractions were combined and frozen at -80 °C followed by subsequent lyophilization. Analytical data for all peptides is collected in Table 3.

## MS/MS

Lyophilized byproducts were dissolved in acetonitrile–water (1 : 1) and diluted 1 : 100. Full scan and product ion spectra were acquired on a LTQ Orbitrap XL ETD (Thermo Scientific) mass spectrometer in the positive ion mode. The sample solutions were infused into the mass spectrometer using a built-in syringe pump at a flow rate of 2 μl min<sup>-1</sup>. The following general parameters were used: spray voltage 1.6 kV, capillary temperature 200 °C, and tube lens voltage 125 V. Collision energies were chosen from 10 to 50 eV and optimized to achieve the desired level of fragmentation. Data acquisition and analysis was performed using Xcalibur software (version 2.0.7, Thermo Scientific). The mass spectrometer was calibrated externally using the manufacturer's calibration standard mixture.

## Cell culture and resazurin-based cell viability assay

MCF-7 human breast adenocarcinoma cells were used for preliminary cytotoxicity studies. They were grown to confluency at 37 °C and 5% CO<sub>2</sub> in a humidified atmosphere in 75 cm<sup>2</sup> cell culture flasks. DMEM/Ham's F12 medium supplemented with 10% heat-

inactivated fetal bovine serum (FBS) (v/v) and 2 mM L-glutamine (Q) was used. The effect of cymantrene peptide conjugate **Cym1-sC18** on the cell viability was examined using a resazurin-based *in vitro* toxicology assay. MCF-7 cells were seeded in 96-well plates at 40,000 cells per well. Having reached 80% confluency, the medium was removed and cells were incubated for 24 h at 37 °C with the test substance at different concentrations. Negative controls were incubated with cell culture medium only. After 24 h, the cells were washed and incubated for 2 h with 10% resazurin in cell medium without fetal bovine serum (v/v) at 37 °C. As a positive control, cells treated with 70% ethanol were used since this is known to be highly toxic to cells. The fluorescence was measured using a Spectrafluor plus multiwell reader (Tecan) at 595 nm with excitation at 550 nm.

## X-ray crystallographic data collection and refinement of structures **Cym3** to **Cym6**

A single crystal of either **Cym3**, **Cym4**, **Cym5**, or **Cym6** was coated with perfluoropolyether, picked up with a glass fiber, and immediately mounted in the nitrogen cold stream of the diffractometer. Intensity data were collected at 213(2) or 223(2) K using graphite monochromated Mo-Kα radiation (λ = 0.71073 Å). Final cell constants were obtained from a least squares fit of a subset of a few thousand strong reflections. Data collection was performed by hemisphere runs taking frames at 0.3° in ω on a Bruker AXS CCD 1000 diffractometer. The program SADABS was used to account for absorption.<sup>35</sup> The SHELXL-97 software package was used for solution, refinement, and artwork of the structures.<sup>36</sup> The structures were readily solved by Patterson methods and difference Fourier techniques. All non-hydrogen atoms were refined anisotropically and hydrogen atoms were placed at calculated positions and refined as riding atoms with isotropic displacement parameters. Note that for **Cym6**, the data completeness is low due to crystal decomposition during the measurement. CCDC numbers: 681218, 744989, 744990, and 744991.†

## Acknowledgements

The authors thank R. Reppich-Sacher for help with the MALDI and ESI mass spectrometry, K. Löbner for help with the cell cultures, and N. Zehethofer (Ultrasensitive Protein Detection Unit, Leipzig University) for help with the MS/MS analysis. This work was supported by the Deutsche Forschungsgemeinschaft (DFG) within the project FOR 630 "Biological function of organometallic compounds". I. N. and U. S. thank Prof. Dr A. G. Beck-Sickinger (Leipzig) and Prof. Dr N. Metzler-Nolte (Bochum) for generous access to all facilities of the respective institutes.

## References

- 1 G. Jaouen, *Bioorganometallics*, Wiley-VCH, Weinheim, 2006.
- 2 D. R. van Staveren and N. Metzler-Nolte, *Chem. Rev.*, 2004, **104**, 5931.
- 3 N. Metzler-Nolte, *Chimia*, 2007, **61**, 736.
- 4 F. Noor, A. Wüstholtz, R. Kinscherf and N. Metzler-Nolte, *Angew. Chem.*, 2005, **117**, 2481.
- 5 S. Mukhopadhyay, C. M. Barnes, A. Haskel, S. M. Short, K. R. Barnes and S. J. Lippard, *Bioconjugate Chem.*, 2008, **19**, 39.
- 6 M. A. Neukamm, A. Pinto and N. Metzler-Nolte, *Chem. Commun.*, 2008, 232.

- 7 J. T. Chantson, M. V. Verga Falzacappa, S. Crovella and N. Metzler-Nolte, *J. Organomet. Chem.*, 2005, **690**, 4564.
- 8 J. T. Chantson, M. V. V. Falzacappa, S. Crovella and N. Metzler-Nolte, *ChemMedChem*, 2006, **1**, 1268.
- 9 D. Zwanziger and A. G. Beck-Sickinger, *Curr. Pharm. Des.*, 2008, **14**, 2385.
- 10 N. Agorastos, L. Borsig, A. Renard, P. Antoni, G. Viola, B. Spingler, P. Kurz and R. Alberto, *Chem.–Eur. J.*, 2007, **13**, 3842.
- 11 A. F. Armstrong, N. Oakley, S. Parker, P. W. Causey, J. Lemon, A. Capretta, C. Zimmerman, J. Joyal, F. Appoh, J. Zubieta, J. W. Babich, G. Singh and J. F. Valliant, *Chem. Commun.*, 2008, 5532.
- 12 K. A. Mahmoud and H. B. Kraatz, *Chem.–Eur. J.*, 2007, **13**, 5885.
- 13 G. Dirscherl and B. König, *Eur. J. Org. Chem.*, 2008, 597.
- 14 S. I. Kirin, P. Dübön, T. Weyhermüller, E. Bill and N. Metzler-Nolte, *Inorg. Chem.*, 2005, **44**, 5405.
- 15 L. Barisic, V. Ropic and N. Metzler-Nolte, *Eur. J. Inorg. Chem.*, 2006, 4019.
- 16 U. Hoffmanns and N. Metzler-Nolte, *Bioconjugate Chem.*, 2006, **17**, 204.
- 17 H. Pfeiffer, A. Rojas, J. Niesel and U. Schatzschneider, *Dalton Trans.*, 2009, 4292.
- 18 I. Neundorf, R. Rennert, J. Hoyer, F. Schramm, K. Löbner, I. Kitanovic and S. Wölf, *Pharmaceuticals*, 2009, **2**, 49.
- 19 Ü. Langel, *Handbook of Cell-Penetrating Peptides*, 2nd edn, CRC Press, Boca Raton, 2006.
- 20 A. Joliot and A. Prochiantz, *Nat. Cell Biol.*, 2004, **6**, 189.
- 21 M. Mäe and Ü. Langel, *Curr. Opin. Pharmacol.*, 2006, **6**, 509.
- 22 K. M. Stewart, K. L. Horton and S. O. Kelley, *Org. Biomol. Chem.*, 2008, **6**, 2242.
- 23 R. Rennert, I. Neundorf, H. G. Jahnke, P. Suchowerskyj, P. Dournaud, A. Robitzki and A. G. Beck-Sickinger, *ChemMedChem*, 2008, **3**, 241.
- 24 C. Walther, K. Meyer, R. Rennert and I. Neundorf, *Bioconjugate Chem.*, 2008, **19**, 2346.
- 25 C. Walther, I. Ott, R. Gust and I. Neundorf, *Biopolymers*, 2009, **92**, 445.
- 26 H. W. Peindy N'Dongo, I. Ott, R. Gust and U. Schatzschneider, *J. Organomet. Chem.*, 2009, **694**, 823.
- 27 H. W. Peindy N'Dongo, I. Neundorf, K. Merz and U. Schatzschneider, *J. Inorg. Biochem.*, 2008, **102**, 2114.
- 28 I. Neundorf, J. Hoyer, K. Splith, R. Rennert, H. W. Peindy N'Dongo and U. Schatzschneider, *Chem. Commun.*, 2008, 5604.
- 29 E. R. Biehl and P. C. Reeves, *Synthesis*, 1973, 360.
- 30 R. A. Firestone, N. S. Maciejewicz and B. G. Christensen, *J. Org. Chem.*, 1974, **39**, 3384.
- 31 E.-D. Chenot, D. Bernardi, A. Comel and G. Kirsch, *Synth. Commun.*, 2007, **37**, 483.
- 32 P. Stathopoulos, S. Papas and V. Tsikaris, *J. Pept. Sci.*, 2006, **12**, 227.
- 33 H. E. Gottlieb, V. Kotlyar and A. Nudelman, *J. Org. Chem.*, 1997, **62**, 7512.
- 34 B. Rist, M. Entzeroth and A. G. Beck-Sickinger, *J. Med. Chem.*, 1998, **41**, 117.
- 35 G. M. Sheldrick, *SADABS, Program for Empirical Correction of Area Detector Data*, (1996), Universität Göttingen, Germany.
- 36 G. M. Sheldrick, *SHELXL-97, Program for Crystal Structure Refinement*, (1997), Universität Göttingen, Germany.